18.06.2019

Re: "Octahedral molybdenum cluster as a photoactive antimicrobial additive to a fluoroplastic" authored by Natalia A. Vorotnikova, Alexander Y. Alekseev, Yuri A. Vorotnikov, Darya V. Evtushok, Yann Molard, Maria Amela-Cortes, Stéphane Cordier, Anton I. Smolentsev, Christian G. Burton, Peter M. Kozhin, Patricia Zhu, Paul D. Topham, Yuri V. Mironov, Bradley, Olga A. Efremova, Michael A. Shestopalov

AUTHOR DECLARATION

We wish to confirm that there are no known conflicts of interest associated with this publication and there has been no significant financial support for this work that could have influenced its outcome.

We confirm that the manuscript has been read and approved by all named authors and that there are no other persons who satisfied the criteria for authorship but are not listed. We further confirm that the order of authors listed in the manuscript has been approved by all of us.

We confirm that we have given due consideration to the protection of intellectual property associated with this work and that there are no impediments to publication, including the timing of publication, with respect to intellectual property. In so doing we confirm that we have followed the regulations of our institutions concerning intellectual property.

We understand that the Corresponding Author is the sole contact for the Editorial process (including Editorial Manager and direct communications with the office). He/she is responsible for communicating with the other authors about progress, submissions of revisions and final approval of proofs. We confirm that we have provided a current, correct email address which is accessible by the Corresponding Author and which has been configured to accept email from o.efremova@hull.ac.uk.

Olga Efremova (on behalf of all authors)

Octahedral molybdenum cluster as a photoactive antimicrobial additive to a fluoroplastic

Natalia A. Vorotnikova,[a,b] Alexander Y. Alekseev,[c] Yuri A. Vorotnikov,[a,b] Darya V. Evtushok,[a,b] Yann Molard,[d] Maria Amela-Cortes,[d] Stéphane Cordier,[d] Anton I. Smolentsev,[a,e] Christian G. Burton,[f] Peter M. Kozhin,[c] Patricia Zhu,[g] Paul D. Topham,[f] Yuri V. Mironov[a,e], Mark Bradley,[g] Olga A. Efremova,[b,c,h] Michael A. Shestopalov[a,b,e]**

[a]Nikolaev Institute of Inorganic Chemistry SB RAS, 3 acad. Lavrentiev ave., 630090 Novosibirsk, Russian Federation.

[b]Research Institute of Clinical and Experimental Lymphology – Branch of the ICG SB RAS, 2 Timakova st., 630060 Novosibirsk, Russian Federation.

[c]Federal Research Centre for Basic and Translational Medicine, 2 Timakova st.,630060 Novosibirsk, Russian Federation.

[d]Institut des Sciences Chimiques de Rennes, Université de Rennes 1, CNRS UMR 6226, Avenue du Général Leclerc, 35042 Rennes, France.

[e]Novosibirsk State University, 2 Pirogova st., 630090 Novosibirsk, Russian Federation

[f]Aston Institute of Materials Research, Aston University, Aston Triangle, B4 7ET Birmingham, United Kingdom.

[g]The School of Chemistry, University of Edinburgh, Kings' Buildings, David Brewster Road, EH9 3FJ Edinburgh, United Kingdom.

[h]Chemistry, Faculty of Science and Engineering, University of Hull, HU6 7RX Hull, United Kingdom.

*Corresponding Authors:

*Olga A. Efremova

Tel: +441482465417, Fax: +441482466410

e-mail: o.efremova@hull.ac.uk.

**Michael A. Shestopalov

Tel. +7-383-330-92-53, Fax +7-383-330-94-89

e-mail: shtopy@niic.nsc.ru

Keywords Octahedral tungsten cluster, anti-bacterial materials, photo-dynamic inactivation.

Abstract Finding methods that fight bacterial infection or contamination, while minimising our reliance on antibiotics is one of the most pressing needs of this century. Although the utilisation of UV-C light and strong oxidising agents, such as bleach, are still efficacious methods for eliminating bacterial surface contamination, both methods present severe health

and/or environmental hazards. Materials with intrinsic photodynamic activity (i.e. a material's ability upon photoexcitation to convert molecular oxygen into reactive oxygen species such as singlet oxygen), which work with light within the visible photomagnetic spectrum could offer a significantly safer alternative. Here we present a new, bespoke molybdenum cluster $(Bu_4N)_2[Mo_6I_8(n\text{-}C_7F_{15}COO)_6]$, which is both efficient in the generation of singlet oxygen upon photoirradiation and compatible with the fluoropolymer (F23-L) known for its good oxygen permeability. Thus, $(Bu_4N)_2[Mo_6I_8(n\text{-}C_7F_{15}COO)_6]$/F23-L mixtures have been solution-processed to give homogenous films of smooth and fibrous morphologies and which displayed high photoinduced antibacterial activity against four common pathogens under visible light irradiation. These materials thus have potential in applications ranging from antibacterial coatings to filtration membranes and air conditioners to prevent spread of bacterial infections.

Introduction

The massive overuse and inappropriate use of antibiotics by healthcare organisations, consumer healthcare industries and agriculture have resulted in the selection of microorganisms resistant to all existing classes of antibiotics [1]. The World Health Organisation (WHO) has named antimicrobial resistance as a grand challenge and called for action to safe-guard existing antibacterial agents, develop new antibacterial and reduce the incidence of infection [2]. The development of new antibiotics is a long and costly process with only few new classes of antibiotics been developed over the last 30 years and the likelihood of a new class appearing any time soon is slim [3].

Therefore, alternative strategies to treat bacterial infections or contaminations need to be developed, if not to substitute existing antibiotic-based technologies, then at least to slow down the spread of resistant bacteria. One alternative method that is currently being explored is based on photodynamic-based inactivation (PDI) [4]. The great benefit of PDI is that it works well on the antibiotic resistant bacteria and (so far) has not been shown to give rise to resistance [5-7]. This approach uses a photoactive compound (a photosensitiser) which, when activated by light, transfers energy to molecular oxygen ($^3O_2$) to generate reactive oxygen species (ROSs), in particular singlet oxygen ($^1O_2$), which is highly reactive and oxidises a broad range of biological molecules resulting in bacterial death.

Highly photoluminescent complexes of the general formula $[\{Mo_6I_8\}L_6]^{2-}$, where L is an electron-withdrawing ligand, in particular perfluorinated carboxylic acid and organic sulfonate, demonstrate the ability to efficiently generate singlet oxygen upon excitation with UV or blue light [8-11], and thus they are good candidates as photosensitisers for materials

with photoinduced antibacterial activity. In a proof-of-concept studies it was demonstrated that compounds based on $\{Mo_6I_8\}^{4+}$ had antibacterial activity against *S. aureus* [12,13] and *E. faecalis [14]*, while in our recent study, silica nanoparticles doped with molybdenum clusters demonstrated pronounced photodynamic activity against larynx carcinoma (Hep2) cells [15].

In developing a new PDI photosensitiser the matrix within which it is supported needs to be considered, needing to be inert to oxidation as well as highly oxygen permeable. Therefore, in this work we challenged ourselves to develop materials based on non-oxidisable fluorinated polymers and the luminescent molybdenum clusters. Importantly fluorinated polymers are well known to have good oxygen permeability and have been used for example, in oxygen sensing applications [16-18] and as an oxygen carrier in artificial blood [19]. Moreover, singlet oxygen tends to have longer lifetimes in fluorinated polymers, since the paucity of C–H and O–H bonds limits unwanted vibrational relaxation of $^1O_2$ to $^3O_2$ [20,21].

The fluoroplastic, F-32L, that was targeted in this work is a copolymer of trifluorochloroethylene and vinylidenedifluoride [–$(CF_2$-$CFCl)_n$-$(CH_2$-$CF_2)_m$–], and is typically used for coating applications. Unlike many other highly fluorinated organic polymers, F-32L can be dissolved in solvents, such as organic esters, and thus can be easily processed by a number of solution-based techniques, including dip-coating, spin-coating, electrospinning and electrospraying. The polymer is also relatively transparent in the UV and blue regions, chemically and thermally stable and hydrophobic. Hydrophobic polymers are being actively used for the development of materials for self-cleaning coatings, as they may have reduced bacterial adhesion [22,23]. Moreover, its poor wettability would ensure protection for the molybdenum cluster complex against hydrolysis a tendency that is well documented [24-28].

To match the solubility of the cluster complexes with those of F-32L within the fluorinated polymer, we designed, synthesised and characterised a new cluster complex $(Bu_4N)_2[\{Mo_6I_8\}(CF_3(CF_2)_6COO)_6]$ that bears long perfluorinated apical ligands to also allow good homogenisation in the fluoroplastic. In combination, these were used to prepare both smooth and fibrous films and evaluated for PDI of both Gram-positive and Gram-negative bacteria.

Experimental section

Materials

$(Bu_4N)_2[\{Mo_6I_8\}I_6]$ was synthesised according to earlier reported procedures [29]. F-32L (butylacetate solution) was purchased from HaloPolymer (Russia). The solvent was

evaporated and the polymer was used without further purification. Other chemical reagents were purchased from Fisher, Aldrich or Alfa Aesar and used as received.

Methods

NMR spectra were recorded on a Bruker 400 MHz Av III spectrometer at 298K. Elemental analyses were performed using a EuroVector EA3000 Elemental Analyser. FTIR spectra were recorded on a Bruker Vertex 80 as KBr disks. Energy-dispersive X-ray spectroscopy (EDS) was performed on a Hitachi TM3000 TableTop SEM with a Bruker QUANTAX 70 EDS equipment with results reported as the ratio of the heavy elements: Mo and I. The relative error of the method was about 5%. Mass spectrometric (MS) detection was performed in negative mode within the 500–4000 m/z range on an electrospray ionization quadrupole time-of-flight (ESI-q-TOF) high-resolution mass spectrometer Maxis 4G (Bruker Daltonics, Germany). The size and morphology of the fibres were characterised by scanning electron microscopy (SEM) using a Zeiss EVO60 Scanning Electron Microscope. The unity of the emission from the fibrous films was characterised using a Zeiss LSM710 Laser Scanning Confocal Microscope equipped with a laser diode (405 nm) for fluorescence and with an APOCHROMAT 63x/1.4 Oil DIC LD Plan objective.

Synthesis of $AgOOC(CF_2)_6CF_3$

Ag_2CO_3 (167 mg, 0.61 mmol) was added to 20 mL of a (1:1) solution of CH_3OH/CH_3CN and *n*-perflurooctanoic acid (550 mg, 1.3 mmol). The mixture was sonicated until CO_2 ceased evolving. The solution was then filtered and the volume of the solution was reduced down to 1 ml on a rotary evaporator. Diethyl ether (20 mL) was added to the oil-like residue and the mixture was kept in a spark free fridge for several hours. The diethyl ether was evaporated leaving white plate-like crystals. Yield: 455 mg (72%). For $C_8AgF_{15}O_2$: calcd: C 18.4. Found: C 18.3; NMR ^{19}F: 95.90-95.71 (3F), 57.85-57.68 (2F), 54.38-55.06 (2F), 55.06-54.72 (2F), 54.3-54.05 (2F), 54.05-53.84 (2F), 50.82-50.59 (2F), IR (KBr, cm^{-1}): 3458 (wk, brd), 3030 (wk), 2964 (wk), 2935 (wk), 2862 (wk), 1614 (str), 1421 (med), 1365 (med), 1325 (med), 1240 (str), 1203 (str), 1145 (str), 1105 (med), 1020 (med), 889 (wk), 821 (med), 771 (wk), 734 (med), 667 (med), 634 (med), 611 (wk), 561 (med), 530 (wk).

Synthesis of $(Bu_4N)_2[\{Mo_6I_8\}(CF_3(CF_2)_6COO)_6]$ (1)

$AgOOC(CF_2)_6CH_3$ (300 mg, 0.57 mmol) was added to the solution of $(Bu_4N)_2[\{Mo_6I_8\}I_6]$ (259 mg, 0.09 mmol) in acetone (20 mL). The reaction mixture was covered in aluminium foil and left to stir for 4 days. The precipitate of AgI formed was removed by filtration and the acetone removed on a rotary evaporator to give an oil-like residue. To obtain clean product, the residue was mixed with ethanol (20 mL), decanted and dried in air. Crystals

suitable for single crystal X-ray structural analysis were obtained by reverse diffusion of diethyl ether from diethyl ether/ethanol solution (1/10) of **1** to pure ethanol. Specifically, they always had small sizes and were shaped as thin plates growing in the form of mille-feuille cake. Yield: 272 mg (66%). For $C_{80}H_{72}F_{90}I_8Mo_6N_2O_{12}$: calcd: C 21.1; H 1.6; N 0.6. Found: C 21.0; H 1.7; N 0.6. EDS: Mo: I ratio of 6 : 8.2; NMR ^{19}F: 95.8-95.6 (3F), 60.25-60.05 (2F), 55.82-55.53 (2F), 55.06-54.72 (2F), 54.55-54.28 (2F), 54.28-53.95 (2F), 50.77-50.55 (2F), IR (KBr, cm^{-1}): 3437 (med, brd), 2974 (med), 2941 (med), 2883 (wk), 2058 (wk), 1695 (srt), 1614 (wk), 1489 (med), 1465 (wk), 1357 (str), 1317 (med), 1240 (str), 1203 (str), 1147 (str), 1014 (med), 885 (wk), 839 (wk), 808 (med), 734 (med), 665 (med), 561 (med), 530 (wk), ESI-MS: M/z For $[\{Mo_6I_8\}(CF_3(CF_2)_6COO)_6]^{2-}$: – 2034.73 (found), 2034.6192 (calculated).

Preparation of $(Bu_4N)_2[\{Mo_6I_8\}(CF_3(CF_2)_6COO)_6]$@F-32L (1@F-32L) materials

Smooth films – To prepare bulk samples containing 0, 0.1, 0.5, 1.0, 5.0 %wt of the cluster, compound **1** was dissolved in butyl acetate (3 ml) under sonication for 30 min and mixed with 3 ml of a butyl acetate solution containing 500 mg of F-32L. The final solution was poured into a Petri dish and left to evaporate under ambient conditions leaving the bulk polymers. Thin films were also prepared by spin-coating. The cluster concentration was 50 mg mL^{-1} with 100 µL of an ethyl acetate solution containing F32-L (50 mg mL^{-1}) layered onto a piece of pre-cleaned glass slide of 1 cm × 1.5 cm and spin coated at 1500 rpm for 2 min using an Ossila spin-coater. The thickness of the films was in the range 40-50 nm as measured by a DektakXT Profiler (Bruker).

Fibrous films - Fibrous films containing 0.1-5 %wt of **1** were obtained by electrospinning. F-32L and compound **1** were separately dissolved in ethyl acetate and the solutions were mixed to give 22 %wt solution of F-32L. A high voltage power supply (Genvolt, 0–30 kV voltage power source, UK) was used to generate the electric field. Flow rates were controlled by a syringe pump (model no. Alladin-8000, World Precision Instruments, UK). Solutions were spun using a blunt steel syringe tip gauge 16 (1.194 mm internal diameter, 36 mm length), which was used as the anode. An aluminium foil flat plate collector (210 mm × 210 mm) was used as the cathode and a target. The prepared solutions were electrospun at constant conditions of 22 kV potential difference, 1.6 mL/h flow rate, and 15 cm distance between the spinning tip and collector plate. The apparatus was enclosed in a Perspex box, and the spinning was performed at approximately 19 ℃ and ambient humidity. The fibrous films were removed from the collector, and stored under dry nitrogen to enable residual solvent evaporation.

Crystallography

Single-crystal X-ray diffraction data were collected at 150 K on a Bruker Nonius X8 Apex 4 K CCD diffractometer fitted with graphite monochromatised MoKα radiation (λ = 0.71073 Å). Absorption corrections were made empirically using the SADABS program [30]. The structures were solved by the direct methods and further refined by the full-matrix least-squares method using the SHELXTL program package [30]. The crystallographic data and details of the structure refinements are summarized in Table S1. CCDC 1896955 contain the supplementary crystallographic data for this paper. These data can be obtained free of charge from the Cambridge Crystallographic Data Centre *via* www.ccdc.cam.ac.uk/data_request/cif. As described above, small thin plate shaped single-crystals grew in stacks leading to difficulty in their separation despite our efforts. Thus, the X-ray diffraction data collection was performed on a twin crystal. The quality of the data did not enable us to reach high quality structural resolution with low values of the reliability factors. The refined formula agrees with the chemical formula determined by several other techniques. Namely, as discussed below, the chemical composition has been determined by the combined use of chemical analyses, NMR and UV-vis spectroscopies. Despite high values of the reliability factors induced by the twinning, the refined X-ray diffraction data afforded a reliable structural model of the cluster complex including the local coordination geometry of the $\{Mo_6I_8\}$-cluster core, the conformation of the perfluorooctanoic terminal ligands, as well as the presence of tetrabutylammonium cations. Moreover bond-lengths and bond-angles of the different groups agree with those already reported in the literature [8,9,11,31].

Photoluminescence measurements

The absolute quantum yields were measured using a C9920–03 Hamamatsu system equipped with a 150 W xenon lamp, a monochromator, an integrating sphere and a red-NIR sensitive PMA-12 detector. Lifetime measurements and TRPL mapping were performed using a picosecond laser diode (Jobin Yvon deltadiode, 375 nm) and a Hamamatsu C10910-25 streak camera mounted with a slow single sweep unit. Signals were integrated on a 30 nm bandwidth. Fits were obtained using ORIGIN software and the goodness of fit was judged by the reduced χ^2 value and residual plot shape. Steady state O_2 ($^1\Delta_g$) measurements were realised with a Hamamatsu H12397-75 NIR-PMT unit mounted on an IHR3 spectrometer. Excitation of a powder sample deposited on quartz substrates or CH_2Cl_2 solution was realised with a 375 nm laser pulsed diode (Jobin Yvon deltadiode). The system was also equipped with a TCSPC unit to measure the emission lifetime.

Stern-Volmer Dependence measurements

The facet of a large-core plastic optical fibre (02-534, Edmund Optics) with a 980 μm core was dip-coated with **1**(5%)@F32-L by dipping into ethyl acetate solutions containing **1**(5%)@F32-L in concentration 4.1 mg/ml and then dried in air for 2 h. The probe was placed into a gas chamber, where the concentration of oxygen in the mixture was controlled by adjusting the partial pressures of O_2 with an additional gas (CO_2), and was calibrated using a commercial paramagnetic oxygen gas analyser (Cardiocap 5, Datex-Ohmeda). The excitation light from a laser source with an emission wavelength of λ = 405 nm (56RCS002, Melles Griot) used at 60 μW was coupled to the opposite, with the proximal fibre facet after being reflected by an angled dichroic mirror. The edge-pass dichroic mirror was chosen such that it was highly transmissive at the emission wavelengths, but highly reflective at the excitation wavelength used. The emission spectra at different concentration of oxygen in the mixtures was measured using a fibre-coupled CCD spectrometer (QE Pro. Ocean Optics). Ten replicates were made for each oxygen concentration point and the average value of integrated intensity between 600 and 800 nm were calculated.

Study of bacterial adhesion on 1@F-32L spin-coated and fibrous films

The bacteria suspension was incubated in 0.1 M carbonate buffer (pH 9.5) containing 1 mg/mL of Fluorescein isothiocyanate (FITC). After 30 min of incubation at 37℃, the FITC-labelled bacteria were washed thoroughly with phosphate-buffered saline (PBS) [32]. 50 μL portions of the bacterial suspensions were then dropped on glass slides (as a control), on glass-slides spin-coated with the polymer sample or on a glass slide covered by a 10×10 mm piece of the fibrous mat and incubated for 30 min at room temperature in a wet chamber. Thereafter, the suspension was carefully decanted. To fix the bacteria, the substrates were immersed into 4% neutral buffered formalin for 10 min. Then the glass slides were imaged and analysed using a standard algorithm in the CellProfiler to determine the number of adhered bacteria [33]. All experiments were performed in triplicate with a confidence interval for P=0.95.

Study of antibacterial activity of 1@F-32L

The antibacterial activity of the materials was tested on *E. coli* (ATCC25922), *S. aureus* (ATCC25923), *S. typhimurium* (ATCC14028) and *P. aeruginosa* (ATCC27853). The bacteria were cultivated in Lysogeny broth (LB) medium at 37℃. The number of viable bacteria was estimated via counting of the colony-forming units (CFU) after 24 h of cultivation. All bacteria cultures had initial concentration of bacteria1-1.2×10^3 in saline. All experiments were performed in triplicate with a confidence interval for P=0.95.

Smooth films – 2.4 ml of the bacterial cultures diluted in saline was evenly distributed in Petri dishes coated with the smooth films of **1**(1%)@F-32L or F-32L. The total thickness of the culture medium with bacteria was about 1 mm. The Petri dishes were irradiated with a UV-lamp OSRAM Germicidal HNS 30W G13 (200-280 nm, 0.12 mW/cm^2) at a distance of 90 cm for 20 min and with a spot light source L8253 (Hamamatsu) at a distance of 20 cm for 10 min (400-800 nm, 220 mW/cm^2). Petri dishes coated with **1**(1%)F-32L were prepared in a similar way but stored in dark for the same time as a negative control. Thereafter the culture media was collected from the Petri dish and cultivated in LB agar culture media. The number of colonies were counted after 24 h.

Fibrous films – 15 µL of bacteria diluted in saline was placed as a single drop on the fibrous films (0.5−1×0.5−1 cm^2) placed on a glass slide or spin coated pieces of glass. The slides were irradiated with a spot light source L8253 (Hamamatsu) at a distance of 10 cm for 20 min. Thereafter the culture media was collected from the films, by placing the film together with the culture media into test tubes and suspending with 400 saline µL for 1 min. Saline with bacteria cultures was used as a negative control. 400 µL of the culture media was collected from the test tube and cultivated in LB agar culture media. The number of colonies were counted after 24 h.

Results and discussion

Synthesis and characterisation of photoactive compound 1

To allow homogenous dispersion of the molybdenum cluster complex in a fluorinated polymer, the cluster complex and the perfluorinated polymer needed to have similar polarity and be soluble in the esters which are typical solvents for F-32L. This match of properties could be achieved by furnishing the molybdenum cluster with long-chain perfluorinated apical ligands. Indeed, experiments with the Bu_4N^+ salts of the known complexes, where L contains only 2 and 3 carbon atoms [9,11,31], have shown that these complexes have rather poor solubility in ester-based solvents. Therefore, to increase the solubility of the cluster a complex with a perfluorooctanoic acid ligand was synthesised following a standard procedure as reported in [9-11,31,34], *i.e.* the reaction of a silver salt of the corresponding acid (6 eq.) with $(Bu_4N)_2[\{Mo_6I_8\}I_6]$. Unlike other molybdenum cluster complexes, compound **1** was soluble in both esters and ethers, for example compound **1** was soluble in ethyl acetate and butyl acetate at 40 mg/ml.

The substitution of all apical iodide ligands $[\{Mo_6I_8\}I_6]^{2-}$ by perfluorooctanate ligands was confirmed by NMR spectroscopy: indeed the ^{19}F NMR spectrum demonstrates only one set

of the signals from the $CF_3(CF_2)_6COO^-$ anion, which is in agreement with the high symmetry of the hexa-substituted complex (Fig. 1). Moreover, there is a significant downfield shift for signals close to carboxylate group in comparison with the free acid, in particular for the fluorine atoms in the α position. These shifts indicate the displacement of the electronic density towards the positively charged metal centre *i.e.* coordination. FTIR spectroscopy further confirms the monodentate mode of the ligand coordination in compound **1**. The vibrations associated with the COO^- group coincide with those for the related compound $(Bu_4N)_2[\{Mo_6I_8\}(n\text{-}C_3F_7COO)_6]$ [11,31] (Fig. S1). Finally, the ESI-MS also indicates a molecular peak that corresponds to $[\{Mo_6I_8\}(CF_3(CF_2)_6COO)_6]^{2-}$ (Fig. S2).

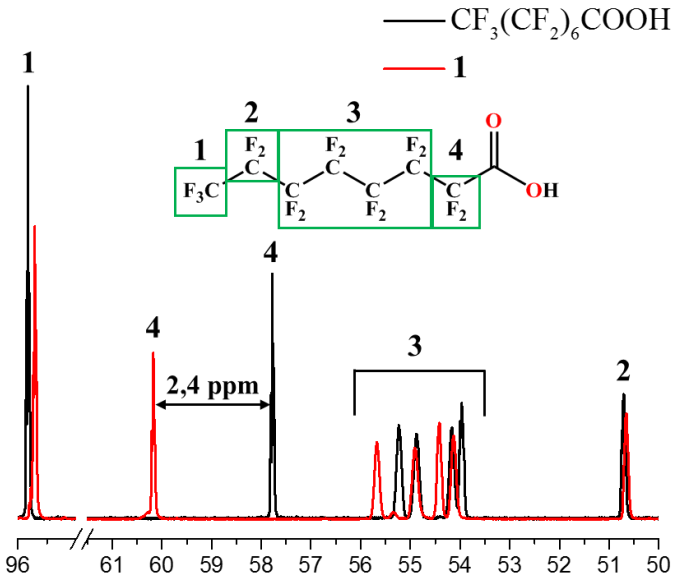

Fig. 1. ^{19}F NMR spectrum of $CF_3(CF_2)_6COOH$ and **1**.

The crystal structure proposal that we obtained agreed well with the formation of cluster compound $(Bu_4N)_2[\{Mo_6I_8\}(CF_3(CF_2)_6COO)_6]$ in the solid state. According to the proposed structure, six $CF_3(CF_2)_6COO^-$ ligands were coordinated to the molybdenum atoms of the cluster core $\{Mo_6I_8\}^{2+}$ through the carboxylic group with bond lengths of about 2.10 Å, similar to those found in related compounds [8,9,11,31]. The perfluorooctanoic ligands orientate along the idealized 3-fold axis as shown in Fig. 2. The anions and tetrabutylammonium cations were packed with the formation of layers containing charged parts of the compound (i.e. the cluster cores and tetrabutylammonium cations) interlayered with interpenetrating perfluroheptyl tails from the ligands. Similar packing was found earlier in the structures of liquid crystal phases based on molybdenum clusters (Fig. 2) [35].

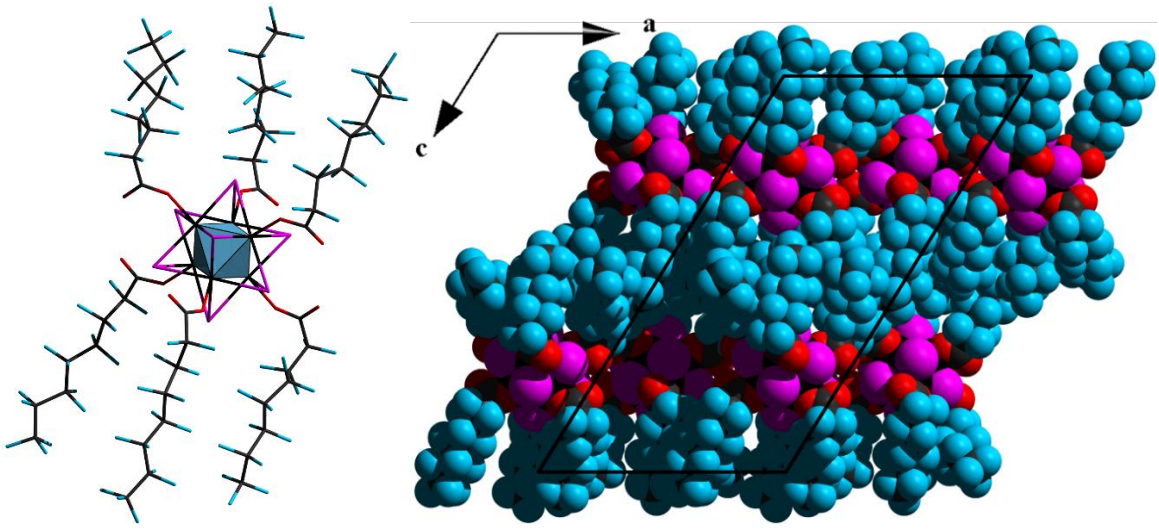

Fig. 2. Structure proposal of the cluster anion $[\{Mo_6I_8\}(CF_3(CF_2)_6COO)_6]^{2-}$ (*left*) and packing of molecules in crystal (*right*) (Bu_4N^+ cations are omitted). Colour code: Mo (black), C (charcoal), O (red), I (magenta), F (light blue), octahedron Mo_6 (blue)

Photoluminescent properties

Similar to other molybdenum cluster complexes coordinated by residues of strong electron withdrawing apical ligands [8-11,31,36,37], compound **1** is a good red emitter and is capable of generating singlet oxygen [8-11]. Specifically, according to the emission-excitation map (Fig. 3), **1** can be excited by wavelengths up to ~475 nm to emit in the region between 600 and 750 nm, with maximum of emission does being invariant to the excitation wavelength.

The photophysical characteristics (maximum intensity of the emission, quantum yields and lifetimes) of powdered and dissolved compound **1** were collected using an excitation wavelength of 375 nm and are summarised in Table 1. Compound **1** demonstrated exceptionally high luminescence quantum yield (0.88) in a deaerated solution, which is similar to other complexes with fluorinated carboxylate ligands [8,11,31].

From Table 1, one can also note that the values of the photoluminescence quantum yield and the lifetimes for compound **1** in both powdered and dissolved state are significantly higher in nitrogen than in air. This is a common feature of octahedral molybdenum cluster complexes and it signifies efficient quenching of the cluster photoluminescence [8-11,31,38,39]. The energy transfer from the excited state of compound **1** to oxygen results in the generation of singlet oxygen ($^1O_2$), as confirmed by the emission spectrum recorded in the region of 1260 nm, *i.e.* at the emission wavelength of $^1\Delta_g$ term of molecular oxygen (Fig. 4).

The lifetime of the singlet oxygen emission was found to be 100 μs when the measurements were taken in a CH_2Cl_2 solution containing compound **1** (Fig. S3). This lifetime is similar to

the value reported earlier for pure CH_2Cl_2 and signifies that the relaxation of singlet oxygen is predominantly due to the interaction with the solvent molecules [21]. The lifetime of singlet oxygen measured in the solid sample of **1** was found to be 46.7 μs, which is the same order of magnitude as for other solid samples [40,41] (Fig. S4).

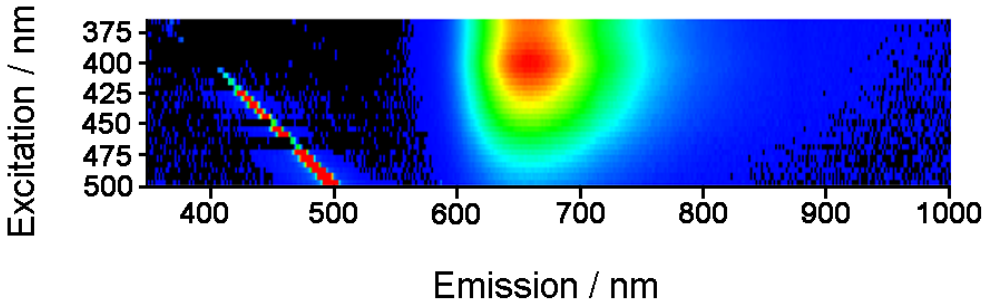

Fig. 3. Emission vs excitation map for deaerated solutions of **1** in CH_2Cl_2. The emission intensity increases from black to red.

Table 1. Photophysical characteristics of compound **1** with an excitation wavelength of 375 nm: λ_{max} – maximum of emission, Φ – photoluminescence quantum yield, τ – luminescence lifetime. The emission intensity increases from black to red.

	λ_{max}, nm	Φ: in air; in nitrogen	τ, μs: in air; in nitrogen	$\tau(^1O_2)$, μs in air
1, powder	~660 nm	0.033; 0.59	10.7; -	100
1, CH_2Cl_2 solution	~660 nm	0.019; 0.88	5.41; 210	46.7

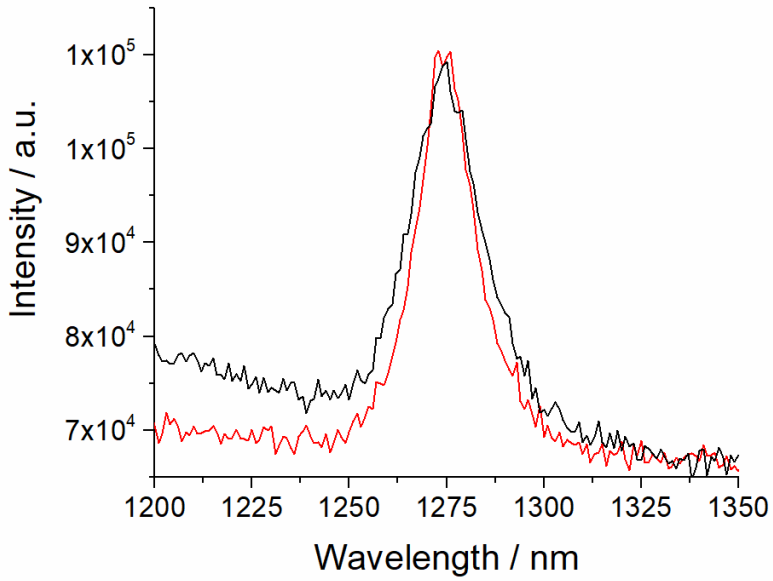

Fig. 4. $^1\Delta_g$ O_2 emission spectra recorded upon irradiating of **1** with an excitation wavelength of 375 nm as a powdered sample (red) or in CH_2Cl_2 solution (black).

To demonstrate that compound **1** still interacts with oxygen while it is within the matrix of F-32L, i.e. diffusion of oxygen through the polymer does not limit the energy transfer to oxygen molecules, luminescence measurements were performed at different concentrations of oxygen in the gas phase. Accordingly, the tip of an unjacketed 980 μm wide core optical fibre was dip-coated in a solution containing 5% of **1** in respect to F-32L. The luminescence spectrum from the coated probe was then recorded in a gas camera at various oxygen concentrations in the mixture. Fig. 5 illustrates a Stern-Volmer plot for the coated optical fibre, i.e. I_0/I vs. oxygen concentration, where I_0 is the integrated intensity of emission in oxygen-free atmosphere, while I is the intensity at the given oxygen percentage [O_2]. The Stern-Volmer plot has an ideal linear dependence with the Stern-Volmer constant K_{SV} = 0.0752 $\%^{-1}$. The linear shape of the Stern-Volmer plot confirms that the quenching by oxygen was not diffusion limited [42].

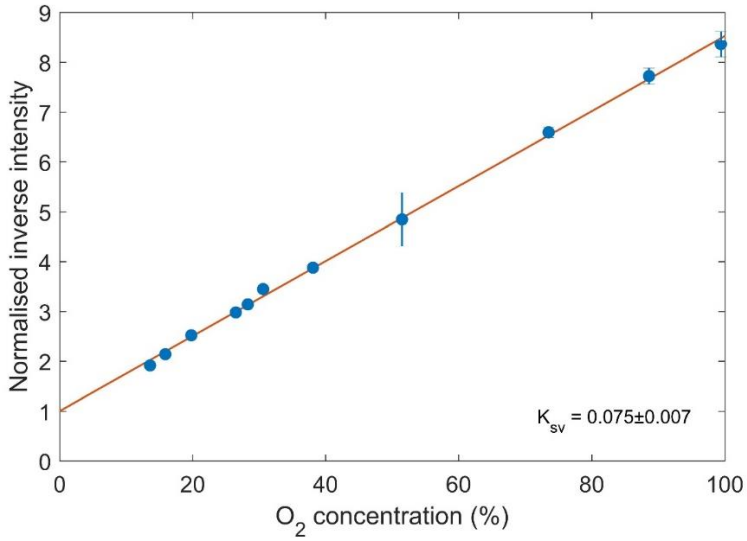

Fig. 5. Normalised inverse intensity signal I_0/I (I_0 is the intensity signal in the absence of oxygen) as function of the oxygen concentration and linear fit to the Stern-Volmer equation, yielding a value of K_{SV} = 0.0752 $\%^{-1}$ of the Stern-Volmer constant.

Preparation of materials 1@F-32L with different morphology

In general, the areas of application of PDI are myriad and include healthcare (infection cure, medical equipment sterilisation, wound care) as well as water/air treatment, packaging, coatings and floor coverings, hygiene products etc. Each application does, however, require a certain formulation and material morphology containing a photosensitiser. Indeed, when preparing materials with antibacterial activity both the surface wettability and the surface texture can affect the adhesion of bacteria. From one side, a rough texture can lead to reduced wettability due to entrapped air and thus reduces the contact area of a water drop that contains

bacterial cultures with the surface and as a consequence a reduced bacterial adhesion [22,23]. On the other hand, a rough surface may allow bacteria to be trapped in the cavities of the material and tallow faster inactivation by the action of singlet oxygen. To demonstrate the appropriateness of the material design to polymer processing and to evaluate the effect of morphology on the antibacterial properties and bacterial adhesion, films of various morphologies were prepared. Owing to the good solubility of both F-32L and compound **1** in esters smooth films and fibrous films (mats) were readily produced.

Smooth films (~0.3 mm thick) were prepared by slow evaporation of butyl-acetate from solutions containing both **1** and F-32L, where the percentage of **1** was set as 0.1, 0.5, 1 and 5 %wt with respect to the polymer matrix. The films appeared as clear yellow transparent plastic materials without any sign of phase separation. Glass-slides coated by films of **1**@F-32L at a thickness of between 40-50 nm were also prepared by spin-coating ethyl acetate solutions at 50 mg mL^{-1} onto pre-cleaned glass slides. The fibrous mats were prepared by electrospinning the ethyl acetate solutions with representative SEM images of the fibrous mats given in Fig. 6. The fibres generally had uneven thickness varying from 0.5-2 μm and also contained some beads with the thickness up to 10 μm. The backscatter SEM images did not reveal any noticeable agglomerates of the cluster within the fibres. Confocal images also confirmed the even distribution of the cluster within the fibres (Fig. S5).

As wettability of the films can be crucial for bacterial adhesion, we compared the contact angles between spin-coated films and electrospun fibres (Fig. S6, Table S2). According to our data the fibres were somewhat more hydrophobic with an average water contact angle of 99.6º (SD=3.74) *vs.* 124º (SD=8.41). This is most likely due to the roughness of the surface that leads to the entrapment of air [22,23]. Notably, the presence of the cluster did not significantly affect the wettability of the materials.

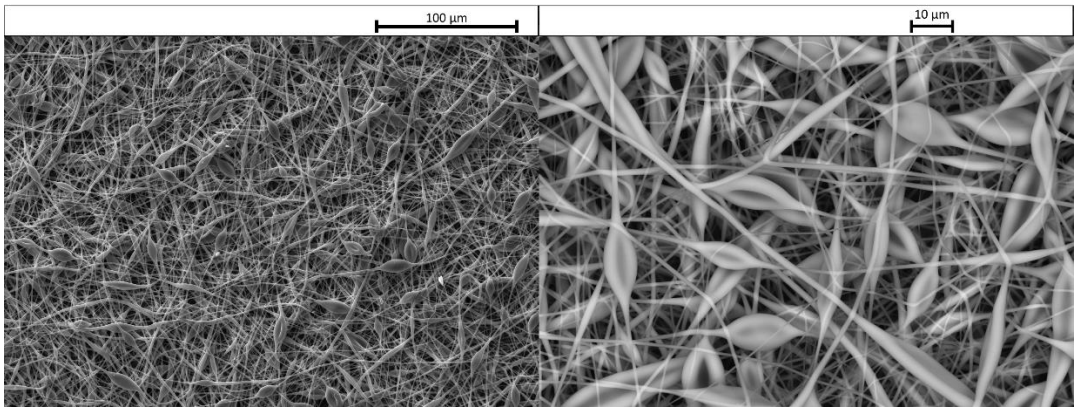

Fig. 6. SEM images of fibrous films **1**(1%)@F-32L.

Bacterial study of the materials

To study the antibacterial potential of both smooth and fibrous materials we evaluated the adhesion of bacteria and their PDI ability. Studies were undertaken on Gram-negative *E. coli*, *S. typhimurium* and *P. aeruginosa* and on Gram-positive *S. aureus* bacteria on the surface of the films. The adhesion of bacterial cultures was studied on both spin-coated films and fibrous mats and compared to adhesion on a glass slide following the method reported earlier. Suspensions of fluorescein-labelled bacteria were placed on the samples of the polymer films or polymer fibres for 30 minutes and then decanted. The polymer samples were imaged by confocal microscopy to estimate the number of remaining (adhered) bacteria. The confocal images (Fig. S7) indicated that bacteria adhered randomly onto the smooth films, while in the case of fibrous materials they adhered (got entrapped) predominantly on the surface of the fibres rather than between the fibres. According to our results (Fig. S8) the bacteria adhesion on the smooth films was comparable with that of glass. In contrast, the adhesion of all types of bacteria, apart from *E.coli* to the fibres was significantly higher than on glass: for example, *P. aeruginosa* and *S. aureus* were up to 12 times more efficient than that on the glass. Notably in both type of materials, fibrous and smooth there seem to be a tendency for the materials with the cluster concentration of 0.1-1 to have slightly higher ability to adhere bacteria for the reasons that are currently not well understood.

PDI activity of the materials was studied for the same bacterial cultures (Fig. S9). Initially, we evaluated the PDI activity of the bulk polymer under a standard UV-C light source irradiation, used for medical sterilisation. (Table 2) Namely, we determined the effect of the presence of the cluster on bacterial growth following photoirradiation, as a percentage reduction of colony-forming units (CFU) in the presence of **1** (1%) in comparison with pristine F-32L for each bacterial culture (GI_{eff}). The presence of **1** reduced CFU of all cultures by 98-99.4%. To confirm that the effect is indeed associated specifically with the PDI activity of the cluster, we also determined the PDI effect (PDI_{eff}) as a percentage reduction of CFU on **1**(1%)@F-32L with and without light irradiation. For all cultures, UV-C irradiation of the material lead to a reduction of CFU by at least 97% or more, which confirms that the antibacterial effect of the cluster is predominantly (if not solely) due to the PDI activity of the cluster.

Table 2. The date on the effect the presence of **1** in the quantity of 1% on bacteria growth upon photoirradiation with UV-C light source and the PDI effect of UV-C light on bacteria growth on bulk **1**(1%)@F32-L.

	Effect of cluster **1** in F-32L on bacteria growth inhibition (GI_{eff}), %	PDI effect of **1**(1%)@F-32L (PDI_{eff}), %
E. coli	98.1±0.8	97.5±1.0
S. aureus	97.9±3.8	99.7±0.2
S. typhimurium	99.4±0.2	99.4±0.3
P. aeruginosa	98.5±0.9	98.5±0.9

[#] $GI_{eff} = \frac{CFU_0 - CFU_1}{CFU_0} \times 100\%$, where CFU_0 is CFU amount on bulk pristine F-32L under light irradiation; CFU_1 is CFU amount on bulk **1**(1%)@F-32L under light irradiation.

[##] $PDI_{eff} = \frac{CFU_1^{light\ off} - CFU_1^{light\ on}}{CFU_1^{light\ off}} \times 100\%$, where $CFU_1^{light\ on}$ is CFU amount on bulk **1**(1%)@F32-L after light irradiation; $CFU_1^{light\ off}$ is CFU amount on bulk **1**(1%)@F32-L without light irradiation.

Having demonstrated the significant PDI activity of the cluster in F-32L polymer, we were keen to evaluate whether light irradiation in the visible range could be used for these purposes as well as the effect that morphology has on the PDI activity. Therefore, the experiments with spin-coated films and electrospun films were undertaken using a white spot-light source (400-800 nm). Our data (Table 3) shows that 0.1% of the cluster in the smooth film was not enough to inactivate any of the cultures, while 0.5% of the cluster in the material inactivates growth of *P. aeruginosa* significantly and *E.coli* and *S. aureus* moderately. 1% of the cluster in the film was sufficient to significantly reduce proliferation of all studied cultures. In regards to the fibrous coatings, 0.1% of the cluster were already sufficient to noticeably inactivate the growth of *P. aeruginosa* and *S aureus*, while 0.5% affected noticeably the growth of all bacteria cultures.

Table 3. The percentage of CFU in comparison to control for spin-coated and fibrous films after irradiation with a white light source. The confidence interval is calculated for P=0.95.

	Content of **1** in F32-L	*E. coli*	*S. aureus*	*S. typhimurium*	*P. aeruginosa*
Spin-coated films	0%	99±9	103±9	101±23	98±15
	0.1%	99±10	102±10	105±20	100±11
	0.5%	61±17	41±7	98±18	15±9
	1%	0.6±0.3	21±3	13±4	3±1
	5%	0.3±0.2	3±2	3±2	0.6±0.3
Fibre films	0%	100±9	99±5	99±13	90±45
	0.1%	100±8	34±3	97±15	19±8
	0.5%	5±1	43±3	10.0±0.9	20±8
	1%	5.7±0.8	43±5	13±1	22±8
	5%	7.7±0.7	34±2	10±1	25±10

To summarise, our bacterial studies demonstrated that the morphology of F-32L was crucial for both adhesion of bacteria and PDI activity. Specifically, bacteria did not have significantly increased adhesion onto smooth films of F-32L, while fibrous films were

capable of entrapping bacteria. On the other hand, the fibrous films required smaller concentration of **1** than smooth films to demonstrate PDI. This is likely due to increased surface area. Thus, smooth **1**@F-32L films have potential for applications as photoactive antibacterial coatings, while fibrous mats may be interesting for applications in water/air purification systems, where such a polymer mesh could be used as a self-sterilising media on exposure to light as a membrane, which is capable of entrapping bacteria. Moreover, polymeric micro/nanofibrous mesh with anti-bacterial activity are also of interest for wound care as the fibrous morphology of the material promote haemostasis, cell respiration, and gas permeation [40,41]

Conclusion

In conclusion, we have developed the first ester/ether soluble, highly phosphorescent molybdenum cluster based compound $(Bu_4N)_2[\{Mo_6I_8\}(CF_3(CF_2)_6COO)_6]$ and demonstrated that it could be used as an additive into fluoropolymer F-32L. Importantly, the hybrid was compatible with solution-based processing/coating techniques including dip-coating, electrospinning and spin-coating. The materials demonstrated a range of useful properties, including good luminescence properties with emission intensities sensitive to oxygen concentration following a linear Stern-Volmer dependence and high PDI activity to all four tested pathogens including *P. aeruginosa* and *S. aureus*, labelled by WHO as of critical priority due to their exceptional antibiotics resistance and importance. Notably, fibrous films have demonstrated significant adhesion of bacteria. Thus, the materials have high potential for numerous applications including optical oxygen sensors, antibacterial coatings and air conditioners as well as reusable self-sterilizing membranes for air, wound and water treatment.

Declarations of interest

None.

Acknowledgments

This work was supported by EPSRC (EP/R006393/1), the Royal Society (RSG\R1\180123) and the Russian Foundation for Basic Research (grant. No. 19-53-12019). This work involved the use of equipment from the Multi-Access Centre “Modern Optical Systems” of the Federal Research Centre for Basic and Translational Medicine.

The raw data required to reproduce these findings are available on request from the authors. The processed data required to reproduce these findings are available to download from [link of ESI will be provided].

Appendix A. Supplementary data

Supplementary data related to this article can be found at https://doi.org/

References

[1] World Health Organization, Antimicrobial Resistance, (2018), https://www.who.int/news-room/fact-sheets/detail/antimicrobial-resistance

[2] World Health Organization, Global Action Plan on Antimicrobial Resistance, (2015), https://www.who.int/antimicrobial-resistance/global-action-plan/en/

[3] A.R.M. Coates, G. Halls, Y.M. Hu, Novel Classes of Antibiotics or More of the Same?, *Br. J. Pharmacol.* **163** (2011) 184-194. https://doi.org/10.1111/j.1476-5381.2011.01250.x

[4] M.R. Hamblin, Antimicrobial Photodynamic Inactivation: a Bright New Technique to Kill Resistant Microbes, *Curr. Opin. Microbiol.* **33** (2016) 67-73. https://doi.org/10.1016/j.mib.2016.06.008

[5] D.M.A. Vera, M.H. Haynes, A.R. Ball, T.H. Dai, C. Astrakas, M.J. Kelso, M.R. Hamblin, G.P. Tegos, Strategies to Potentiate Antimicrobial Photoinactivation by Overcoming Resistant Phenotypes, *Photochem. Photobiol.* **88** (2012) 499-511. https://doi.org/10.1111/j.1751-1097.2012.01087.x

[6] T. Maisch, Resistance in Antimicrobial Photodynamic Inactivation of Bacteria, *Photochem. Photobiol. Sci.* **14** (2015) 1518-1526. https://doi.org/10.1039/c5pp00037h

[7] F. Giuliani, M. Martinelli, A. Cocchi, D. Arbia, L. Fantetti, G. Roncucci, In Vitro Resistance Selection Studies of RLP068/Cl, a New Zn(II) Phthalocyanine Suitable for Antimicrobial Photodynamic Therapy, *Antimicrob. Agents Chemother.* **54** (2010) 637-642. https://doi.org/10.1128/Aac.00603-09

[8] K. Kirakci, P. Kubát, J. Langmaier, T. Polívka, M. Fuciman, K. Fejfarová, K. Lang, A Comparative Study of the Redox and Excited State Properties of $(^{n}Bu_4N)_2[Mo_6X_{14}]$ and $(^{n}Bu_4N)_2[Mo_6X_8(CF_3COO)_6]$ (X = Cl, Br, or I), *Dalton Trans.* **42** (2013) 7224-7232. https://doi.org/10.1039/C3DT32863E

[9] K. Kirakci, P. Kubát, M. Dušek, K. Fejfarová, V. Šícha, J. Mosinger, K. Lang, A Highly Luminescent Hexanuclear Molybdenum Cluster – A Promising Candidate toward

Photoactive Materials, *Eur. J. Inorg. Chem.* (2012) 3107-3111. https://doi.org/10.1002/ejic.201200402

[10] O.A. Efremova, Y.A. Vorotnikov, K.A. Brylev, N.A. Vorotnikova, I.N. Novozhilov, N.V. Kuratieva, M.V. Edeleva, D.M. Benoit, N. Kitamura, Y.V. Mironov, M.A. Shestopalov, A.J. Sutherland, Octahedral Molybdenum Cluster Complexes with Aromatic Sulfonate Ligands, *Dalton Trans.* **45** (2016) 15427-15435. https://doi.org/10.1039/C6DT02863B

[11] M.A. Mikhailov, K.A. Brylev, P.A. Abramov, E. Sakuda, S. Akagi, A. Ito, N. Kitamura, M.N. Sokolov, Synthetic Tuning of Redox, Spectroscopic, and Photophysical Properties of $\{Mo_6I_8\}^{4+}$ Core Cluster Complexes by Terminal Carboxylate Ligands, *Inorg Chem* **55** (2016) 8437-8445. https://doi.org/10.1021/acs.inorgchem.6b01042

[12] A. Beltrán, M. Mikhailov, M.N. Sokolov, V. Pérez-Laguna, A. Rezusta, M.J. Revillo, F. Galindo, A photobleaching Resistant Polymer Supported Hexanuclear Molybdenum Iodide Cluster for Photocatalytic Oxygenations and Photodynamic Inactivation of Staphylococcus Aureus, *J. Mater. Chem. B* **4** (2016) 5975-5979. https://doi.org/10.1039/c6tb01966h

[13] C. Felip-León, C.A. del Valle, V. Perez-Laguna, M.I. Millán-Lou, J.F. Miravet, M. Mikhailov, M.N. Sokolov, A. Rezusta-López, F. Galindo, Superior Performance of Macroporous Over Gel Type Polystyrene as a Support for the Development of Photo-Bactericidal Materials, *J. Mater. Chem. B* **5** (2017) 6058-6064. https://doi.org/10.1039/c7tb01478c

[14] K. Kirakci, J. Zelenka, M. Rumlová, J. Cvačka, T. Ruml, K. Lang, Cationic Octahedral Molybdenum Cluster Complexes Functionalized with Mitochondria-Targeting Ligands: Photodynamic Anticancer and Antibacterial Activities, *Biomater. Sci.* **7** (2019) 1386-1392. https://doi.org/10.1039/c8bm01564c

[15] A.O. Solovieva, Y.A. Vorotnikov, K.E. Trifonova, O.A. Efremova, A.A. Krasilnikova, K.A. Brylev, E.V. Vorontsova, P.A. Avrorov, L.V. Shestopalova, A.F. Poveshchenko, Y.V. Mironov, M.A. Shestopalov, Cellular Internalisation, Bioimaging and Dark and Photodynamic Cytotoxicity of Silica Nanoparticles Doped by $\{Mo_6I_8\}^{4+}$ Metal Clusters, *J. Mater. Chem. B* **4** (2016) 4839-4846. https://doi.org/10.1039/C6TB00723F

[16] R.A. Pasternak, M.V. Christensen, J. Heller, Diffusion and Permeation of Oxygen, Nitrogen, Carbon Dioxide, and Nitrogen Dioxide through Polytetrafluoroethylene, *Macromolecules* **3** (1970) 366-371. https://doi.org/10.1021/ma60015a020

[17] F.W. Giacobbe, Oxygen Permeability of Teflon-PFA Tubing, *J. Appl. Polym. Sci.* **39** (1990) 1121-1132. https://doi.org/10.1002/app.1990.070390508

[18] P.M. Bhadha, How Weld Hose Materials Affect Shielding Gas Quality, *Weld. J.* **78** (1999) 35-40.

[19] S. Moradi, A. Jahanian-Najafabadi, M.H. Roudkenar, Artificial Blood Substitutes: First Steps on the Long Route to Clinical Utility, *Clin. Med. Insights: Blood Disorders* **9** (2016) 33-41. https://doi.org/10.4137/Cmbd.S38461

[20] G. Ghosh, M. Minnis, A.A. Ghogare, I. Abramova, K.A. Cengel, T.M. Busch, A. Greer, Photoactive Fluoropolymer Surfaces That Release Sensitizer Drug Molecules, *J. Phys. Chem. B* **119** (2015) 4155-4164. https://doi.org/10.1021/acs.jpcb.5b00808

[21] K.I. Salokhiddinov, I.M. Byteva, G.P. Gurinovich, Lifetime of Singlet Oxygen in Various Solvents, *J. Appl. Spectrosc.* **34** (1981) 561–564. https://doi.org/10.1007/BF00613067

[22] S.T. Yohe, J.D. Freedman, E.J. Falde, Y.L. Colson, M.W. Grinstaff, A Mechanistic Study of Wetting Superhydrophobic Porous 3D Meshes, *Adv. Funct. Mater.* **23** (2013) 3628-3637. https://doi.org/10.1002/adfm.201203111

[23] A. Lafuma, D. Quere, Superhydrophobic states, *Nat. Mater.* **2** (2003) 457-460. https://doi.org/10.1038/nmat924

[24] K. Kirakci, P. Kubát, M. Kučeráková, V. Šícha, H. Gbelcová, P. Lovecká, P. Grznárová, T. Ruml, K. Lang, Water-Soluble Octahedral Molybdenum Cluster Compounds $Na_2[Mo_6I_8(N_3)_6]$ and $Na_2[Mo_6I_8(NCS)_6]$: Syntheses, Luminescence, and In Vitro Studies, *Inorg. Chim. Acta* **441** (2016) 42-49. https://doi.org/10.1016/j.ica.2015.10.043

[25] Y.A. Vorotnikov, O.A. Efremova, N.A. Vorotnikova, K.A. Brylev, M.V. Edeleva, A.R. Tsygankova, A.I. Smolentsev, N. Kitamura, Y.V. Mironov, M.A. Shestopalov, On the Synthesis and Characterisation of Luminescent Hybrid Particles: Mo_6 Metal Cluster Complex/SiO_2, *RSC Adv.* **6** (2016) 43367-43375. https://doi.org/10.1039/C6RA04321F

[26] M.A. Mikhailov, A.L. Gushchin, M.R. Gallyamov, A.V. Virovets, M.N. Sokolov, D.G. Sheven, V.V. Pervukhin, Tosylate Cluster Complexes $(Bu_4N)_2[M_6I_8(O_3SC_6H_4CH_3)_6]$ (M = Mo, W), *Russ J Coord Chem* **43** (2017) 172-180. https://doi.org/10.1134/S107032841702004x

[27] E.V. Svezhentseva, Y.A. Vorotnikov, A.O. Solovieva, T.N. Pozmogova, I.V. Eltsov, A.A. Ivanov, D.V. Evtushok, S.M. Miroshnichenko, V.V. Yanshole, C.J. Eling, A.M. Adawi, J.S.G. Bouillard, N.V. Kuratieva, M.S. Fufaeva, L.V. Shestopalova, Y.V. Mironov, O.A. Efremova, M.A. Shestopalov, From Photoinduced to Dark Cytotoxicity through an Octahedral Cluster Hydrolysis, *Chem. Eur. J.* **24** (2018) 17915-17920. https://doi.org/10.1002/chem.201804663

[28] M.A. Mikhaylov, P.A. Abramov, V.Y. Komarov, M.N. Sokolov, Cluster Aqua/Hydroxocomplexes Supporting Extended Hydrogen Bonding Networks. Preparation and Structure of a Unique Series of Cluster Hydrates $[Mo_6I_8(OH)_4(H_2O)_2]*nH_2O$ (n=2, 12, 14), *Polyhedron* **122** (2017) 241-246. https://doi.org/10.1016/j.poly.2016.11.011

[29] K. Kirakci, S. Cordier, C. Perrin, Synthesis and Characterization of $Cs_2Mo_6X_{14}$ (X= Br or I)Hexamolybdenum Custer Halides: Efficient Mo-6 Cluster Precursors for Solution Chemistry Syntheses, *Z Anorg Allg Chem* **631** (2005) 411-416. https://doi.org/10.1002/zaac.200400281

[30] *Bruker, APEX2 (Version 1.08), SAINT (Version 7.03), SADABS (Version 2.11), SHELXTL(Version 6.12), Bruker AXS Inc., Madison, WI, USA, 2004.*

[31] M.N. Sokolov, M.A. Mihailov, E.V. Peresypkina, K.A. Brylev, N. Kitamura, V.P. Fedin, Highly luminescent complexes $[Mo_6X_8(n\text{-}C_3F_7COO)_6]^{2-}$ (X = Br, I), *Dalton Trans.* **40** (2011) 6375-6377. https://doi.org/10.1039/c1dt10376h

[32] P. Utaisincharoen, W. Kespichayawattana, N. Anuntagool, P. Chaisuriya, S. Pichyangkul, A.M. Krieg, S. Sirisinha, CpG ODN Enhances Uptake of Bacteria by Mouse Macrophages, *Clin. Exp. Immunol.* **132** (2003) 70-75. https://doi.org/10.1046/j.1365-2249.2003.02107.x

[33] T.R. Jones, I.H. Kang, D.B. Wheeler, R.A. Lindquist, A. Papallo, D.M. Sabatini, P. Golland, A.E. Carpenter, CellProfiler Analyst: Data Exploration and Analysis Software for Complex Image-Based Screens, *Bmc Bioinformatics* **9** (2008) 482. https://doi.org/10.1186/1471-2105-9-482

[34] O.A. Efremova, M.A. Shestopalov, N.A. Chirtsova, A.I. Smolentsev, Y.V. Mironov, N. Kitamura, K.A. Brylev, A.J. Sutherland, A Highly Emissive Inorganic Hexamolybdenum Cluster Complex as a Handy Precursor for the Preparation of New Luminescent Materials, *Dalton Trans.* **43** (2014) 6021-6025. https://doi.org/10.1039/c3dt53126k

[35] Y. Molard, Clustomesogens: Liquid Crystalline Hybrid Nanomaterials Containing Functional Metal Nanoclusters, *Accounts Chem. Res.* **49** (2016) 1514-1523. https://doi.org/10.1021/acs.accounts.6b00236

[36] S. Akagi, S. Fujii, N. Kitamura, A Study on the Redox, Spectroscopic, and Photophysical Characteristics of a Series of Octahedral Hexamolybdenum(II) Clusters: $[\{Mo_6X_8\}Y_6]^{2-}$ (X, Y = Cl, Br, or I), *Dalton Trans.* **47** (2018) 1131-1139. https://doi.org/10.1039/c7dt04485b

[37] N.A. Vorotnikova, Y.A. Vorotnikov, I.N. Novozhilov, M.M. Syrokvashin, V.A. Nadolinny, N.V. Kuratieva, D.M. Benoit, Y.V. Mironov, R.I. Walton, G.J. Clarkson, N.

Kitamura, A.J. Sutherland, M.A. Shestopalov, O.A. Efremova, 23-Electron Octahedral Molybdenum Cluster Complex $[\{Mo_6I_8\}Cl_6]^-$, *Inorg Chem* **57** (2018) 811-820. https://doi.org/10.1021/acs.inorgchem.7b02760

[38] O.A. Efremova, K.A. Brylev, Y.A. Vorotnikov, L. Vejsadova, M.A. Shestopalov, G.F. Chimonides, P. Mikes, P.D. Topham, S.J. Kim, N. Kitamura, A.J. Sutherland, Photoluminescent Materials Based on PMMA and a Highly-Emissive Octahedral Molybdenum Metal Cluster Complex, *J Mater Chem C* **4** (2016) 497-503. https://doi.org/10.1039/c5tc03204k

[39] M. Amela-Cortes, S. Paofai, S. Cordier, H. Folliot, Y. Molard, Tuned Red NIR Phosphorescence of Polyurethane Hybrid Composites Embedding Metallic Nanoclusters for Oxygen Sensing, *Chem. Commun.* **51** (2015) 8177-8180. https://doi.org/10.1039/c5cc01867f

[40] K. Schiller, F.W. Muller, Singlet Oxygen Lifetime in Polymer-Films, *Polym. Int.* **25** (1991) 19-22. https://doi.org/10.1002/pi.4990250105

[41] S. Jockusch, J. Sivaguru, N.J. Turro, V. Ramamurthy, Direct Measurement of the Singlet Oxygen Lifetime in Zeolites by Near-IR Phosphorescence, *Photochem. Photobiol. Sci.* **4** (2005) 403-405. https://doi.org/10.1039/b501701g

[42] J.R. Lakowicz, Quenching of Fluorescence, in: *Principles of Fluorescence Spectroscopy*, 3 ed.; Springer US(2006), pp. 277-330